Nuclear Engineering and Design 417 (2024) 112822

Contents lists available at ScienceDirect

Nuclear Engineering and Design

journal homepage: www.elsevier.com/locate/nucengdes

Numerical and experimental analysis of cylindrical-type PAR catalyst behaviour

A.A. Malakhov [a,*], A.V. Avdeenkov [a,b], M.H. du Toit [c], Q.H. Duong [d], D.G. Bessarabov [a,*]

[a] DST Hydrogen Infrastructure Center of Competence (HySA Infrastructure), Faculty of Engineering, North-West University, Private Bag X6001, Potchefstroom 2520, South Africa
[b] All-Russian Research Institute for Nuclear Power Plants Operation (VNIIAES), Ferganskaya St., 25, Moscow 109507, Russia
[c] School of Mechanical Engineering, Faculty of Engineering, North-West University, Private Bag X6001, Potchefstroom 2520, South Africa
[d] Obninsk Institute for Nuclear Power Engineering of NRNU «MEPhI», Studgorodok St., 1, Obninsk 249040, Russia

ARTICLE INFO

Keywords:
Passive autocatalytic recombiner
Computation fluid dynamics
Hydrogen safety
Catalytic hydrogen combustion
Modelling

ABSTRACT

Passive autocatalytic recombiners (PARs) are essential safety systems used in nuclear power plants (NPPs) to prevent hydrogen explosions during severe accidents. This study investigates the operational behaviour of cylindrical-type catalysts used in a PAR. The study employs experimental and computational fluid dynamics (CFD) analyses to evaluate the catalyst temperature distribution and hydrogen conversion inside the PAR channel. Experimental analysis measures the hydrogen conversion of the catalyst and temperature distribution by means of hydrogen sensors and an infrared camera. The CFD analysis uses a three-dimensional (3D) model developed in STAR-CCM+ code to simulate the flow and recombination reaction in a cylindrical-type PAR catalyst section. Results indicated that the catalyst has decent conversion efficiency. Furthermore, the temperature over the catalyst section is evenly distributed and it does not exceed the lower hydrogen ignition limit. CFD analysis of the Schmidt number demonstrates that the flow inside the PAR is highly turbulent and Sc_t values is in the range of 0.2–0.28. It was found that the recombination reaction occurs in the diffusion regime. The recombination reaction primarily occurs in the catalyst's lower and central parts. Finally, this paper proposes the functional dependence to estimate the efficiency of the entire PAR based on the Sherwood equation and mechanistic transport approach. The results of this study provide crucial insight into the cylindrical-type catalyst operational behaviour in PARs and the CFD model design of cylindrical-type catalysts for the safety analysis of NPPs.

1. Introduction

Over the years, population growth and energy demand have presented the scientific community with major concerns (Abe et al., 2019). Although advanced materials and renewable energy sources show promise to alleviate this in the near future, fossil fuel sources currently dominate electricity production worldwide. The combustion of fossil fuels results in the release of large amounts of greenhouse gases—this is expected to continue to increase. According to a recent report of the International Energy Agency (IEA) in 2019, nearly 27 % of the world's electricity was generated from renewable sources, including hydro, solar, wind, biofuels, waste and others (IEA, 2020). This percentage is projected to increase to 45 % by 2040, demonstrating progress in the development of renewable energy and offering hope that the use of fossil fuels can be reduced, ultimately leading to a reduction in human impact on the environment.

Scientists in the energy field are focused on discovering alternative energy sources to replace fossil fuels. Future energy sources must meet certain criteria, including suitability for transportation, ease of conversion into other forms of energy, high utilisation efficiency, safety throughout the fuel life cycle, environmental friendliness, and affordability. Hydrogen energy is regarded as one of the most promising future energy carriers as it satisfies many desirable characteristics (Maestre et al., 2021). The global production of hydrogen is growing rapidly, leading to a greater need for research into hydrogen production, storage, transportation and utilisation. Nuclear energy is another sustainable and clean technology (du Toit and Chirayath, 2015; du Toit and Naicker, 2018; Rehm, 2023). Despite its potential, hydrogen safety remains to be further studied in terms of possible hydrogen accident scenarios, such as

* Corresponding authors.
E-mail addresses: alexander.malakhov@nwu.ac.za (A.A. Malakhov), dmitri.bessarabov@nwu.ac.za (D.G. Bessarabov).

https://doi.org/10.1016/j.nucengdes.2023.112822
Received 24 July 2023; Received in revised form 20 November 2023; Accepted 5 December 2023
Available online 12 December 2023

Nomenclature

Abbreviations

2D	two dimensional
3D	three dimensional
AECL	Atomic Energy of Canada Ltd.
CFD	computational fluid dynamics
CHC	catalytic hydrogen combustion
DFT	density functional theory
DOM	discrete ordinates method
PAR	passive autocatalytic recombiner
Pt/AAO	platinum/anodic aluminium oxide
NPP	nuclear power plant
STP	standard temperature and pressure
SS	stainless-steel
HPCM	high-porosity ceramic material
RSTS	recombiner sections testing station
RANS	Reynolds-Averaged Navier-Stokes
IR	infrared camera
LFL	lower flammability limit
LES	Large-Eddy Simulation

Symbols

A	pre-exponential coefficient
β	temperature coefficient
C[H_2]	volume H_2 concentration, vol.%
D/D_{im}	molecular diffusion coefficient, m^2/s
D	hydraulic diameter, m
E_a	activation energy
T	temperature, °C
P_0	pressure, kPa
ṁ inlet	mass flow rate, g/min
Y_{H2} H_2	conversion rate, %
ΔC_M	mole fraction of H_2
C_M^{in}	molar concentration of H_2, mol/m^3
R	conversion rate of H_2, g/s
R_u	universal gas constant, $m^2\ kg\ s^{-2}\ K^{-1}\ mol^{-1}$
Re	Reynolds number
S_h	Sherwood number
Sc_t	Schmidt number
w	flow rate, g/s
ν	kinematic viscosity, m^2/s
k_j	reaction rate, $kmol/m^2 \bullet s$

release/leakage, and consequent ignition and detonation (Gardner et al., 2021; Huang et al., 2011; Liang et al., 2016; Malakhov et al., 2020a).

During a hypothetical case of a severe accident in a nuclear power plant (NPP), the steam in contact with zirconium-based cladding in the reactor core can generate a large amount of hydrogen, which can migrate into the containment (Brachet et al., 2014; Paladino et al., 2012). If the low flammability limit of hydrogen in air at STP (4 vol%) is reached, the hydrogen–air mixture can pose a significant danger of deflagration or explosion (du Toit et al., 2018; Kozhukhova et al., 2021a). In the field of NPPs, passive autocatalytic recombiners (PARs) are devices that can mitigate the hazard of hydrogen release in the NPP containment during an accident (such as a loss-of-coolant accident).

Several research institutions, including AECL (Canada) (Sitar et al., 1997), Becker Technologies (Germany) (Gupta et al., 2015), Forschungszentrum Jülich (Germany) (Reinecke et al., 2004) have designed and operated different types of PAR experimental facilities. These facilities have demonstrated the effectiveness of PARs for hydrogen safety applications. Small-scale facilities (or micro-reactors) continue to be widely used in various areas of scientific research. Such test facilities have been identified as most suitable for the study of chemical reactions, especially in catalytic hydrogen combustion (CHC) (Klauck et al., 2014; Steffen et al., 2017).

PAR operation is based on the principle of the exothermic reaction of H_2/O_2 on a catalytic material (noble metals, such as platinum and palladium) (Prabhudharwadkar et al., 2011). The H_2/O_2 recombination reaction can be presented as follows:

$$2H_2 + O_2 = 2H_2O + 244.9kJ/mol$$

The numerical modelling of CHC, in detail, presents a significant computational challenge. The autocatalytic hydrogen recombination process is a multi-stage mechanism. The detailed chemical mechanism may contain different numbers of reactions (12–16), depending on the purpose of the study (Avdeenkov et al., 2018). Many research groups have developed the concept of a detailed chemical kinetic mechanism that takes into account surface- and gas-phase chemistry. Computational fluid dynamics (CFD) is numerical approach used to solve challenging problems related to fluid mechanics, heat transfer, chemical reactions, etc. The advent of CFD offers a significant advancement in studying the progress of chemical processes using the principles of similitude theory, and modelling of heat and mass transfer (Orszulik et al., 2015; Rozeń, 2015a). Several CFD codes, such as ANSYS Fluent, CFX, STAR-CCM+, and others, are being used in engineering numerical simulations (Klauck et al., 2014; Malakhov et al., 2023). CFD offers numerous benefits, such as enabling in-depth analysis of experimental results and extending the investigation to parameters that cannot be tested experimentally. CFD codes can address complex problems related to the flow of fluids or solids, homogeneous and heterogeneous chemical reactions, heat transfer, radiation, electrochemistry, solid stress, laminar and turbulent flow.

Worldwide, many NPPs have installed PARs, manufactured by various companies, including Atomic Energy of Canada Ltd. (Canada), AREVA/Siemens (France, Germany), NIS (Germany), and ISPC Russian Energy Technologies (Russia). Most of these PARs have been studied, in different experimental and numerical works, with different initial conditions; however, the PAR FR-90 manufactured by AREVA (France) has attracted the most research attention (Gera et al., 2010; Prabhudharwadkar et al., 2011; Raman et al., 2020; Shukla et al., 2021).

The aim of this study is to investigate the operational behaviour of a single section of a cylindrical-type PAR catalyst (RVK-500) under defined initial conditions. Specifically, this study seeks to evaluate hydrogen conversion and temperature distribution over the catalyst section through experimental and CFD analyses. A detailed CFD model of H_2/O_2 recombination on a Pt catalyst, based on a conjugated reaction kinetics approach, is proposed. This work also aims to perform the numerical analysis of the kinetics of the hydrogen recombination reaction and mass transfer inside the PAR channel in the case of a single catalytic section, as well as the study of turbulent Schmidt number. The final objective is to contribute to CFD modelling design and optimisation of PAR systems for hydrogen safety.

2. State of the art: diversity of PAR catalysts

PARs are extensively used to mitigate the potential danger of the formation of flammable mixtures after hydrogen release accidents (Kim et al., 2020). A PAR is a vertical flow channel that allows incoming hydrogen from the bottom to pass through the catalytic sections and the products to be released from the top. A PAR consists of a vertical channel that is equipped with catalytic elements in the lower part, assembled into the catalytic block. These catalytic elements can be of various geometric shapes and materials, depending on the manufacturer and the country of use (Arnould et al., 2001). The main materials used in PAR

catalytic elements may be divided into four groups (Kozhukhova et al., 2021b): (i) metallic plate coated with catalyst powder without an intermediate ceramic coating, (ii) cartridges filled with ceramic spherical Pd-coated pellets, (iii) a thin stainless steel (SS) plate wash-coated with a ceramic layer that supports a noble metal (plate-type catalyst), and (iv) γ-Al_2O_3 cylinders wash-coated with a noble metal (cylindrical-type catalyst). Table 1 summarises PAR manufacturers and the accommodated catalyst.

Korea Nuclear Technology Inc. has recently introduced an innovative PAR system featuring a highly porous catalyst material shaped like a honeycomb. This honeycomb PAR catalyst possesses a unique design feature that enhances hydrogen removal performance by simultaneously increasing the surface area and improving the flow rate through the catalyst. Importantly, this performance boost is achieved without enlarging the PAR's size in comparison to conventional PARs. In the tailored Integral Test Facility and Performance Test Facility, two different PAR sizes, namely KPAR-40 and KPAR-T2, were examined. These facilities were used to assess hydrogen depletion rates under various conditions, including different levels of pressure, temperature, and hydrogen concentration, using both a prototype PAR and a scaled test PAR (Kim et al., 2015; Park et al., 2011).

NIS PAR contains flat rectangular cartridges filled with porous spherical ceramic pellets, which are coated with palladium (Pd). A prototype PAR developed by the NIS Company was investigated by Blanchat and Malliakos (1999, 2000). A full-loaded recombiner contains a row of 88 catalytic cartridges; the tests were conducted within different scales of full recombiner loading (1/2, 1/4, 1/8). The PAR catalyst was investigated in a hot and steamy atmosphere (102 °C and 50 mol.% water vapour). Results showed that the PAR commenced operation after 10 min of hydrogen exposure at $C_{in}[H_2] = 1$–6 vol%. The catalyst temperature increased by 96 K for each 1 vol% hydrogen concentration. Hydrogen combustion was observed at low hydrogen concentrations (4–5 vol%), and with peak catalyst temperatures in the range 600–800 K.

Research and development efforts pertaining to advanced catalyst support materials are being conducted by different laboratories, worldwide. In a recent study, Kozhukhova et al. developed the Pt/AAO (Anodic Aluminium Oxide) catalyst for PAR application (Kozhukhova et al., 2019; Kozhukhova et al., 2020; du Preez et al., 2022). The Al/AAO support was prepared by two-step anodization of Al6082 alloy. The Pt/AAO catalyst was prepared by the wet incipient impregnation method. In their investigations, the Pt/AAO catalyst was found to be highly stable over a prolonged hydrogen recombination reaction time of 530 h. The authors determined that hydrogen conversion was almost complete (~95 %). Furthermore, due to the high thermal conductivity of the Al/AAO support, the heat produced during the exothermic hydrogen recombination reaction was displaced from the AAO to the Al core, and the maximum catalyst surface temperature of approximately 210 °C was achieved at 3 vol% of inlet H_2 (Kozhukhova et al., 2021a).

Pt catalysts are predominantly used in PARs, however, it has been observed that Pt catalysts can experience deactivation in the presence of water, leading to a delay in the H_2/O_2 recombination reaction. Therefore, researchers are exploring alternative catalysts that not only reduce the Pt content but also minimise the delay in catalyst initialisation. Recent studies employing density functional theory (DFT) have found that Pt–Ni and Pt–Co alloys exhibit higher catalytic activity in the H_2/O_2 recombination reaction compared to pristine Pt catalysts (Botha et al., 2023).

Table 1
PARs developed for NPPs.

Manufacturer	Catalyst material
Atomic Energy of Canada Ltd. (Canada)	Stainless-steel plate coated with noble metal (Gardner and Marcinkowska, 2012)
AREVA/Siemens (France, Germany)	Stainless-steel plate wash coated with a ceramic layer that supports a noble metal (Reinecke et al., 2004)
Korea Nuclear Technology, Inc. (Republic of Korea)	Ceramic honeycomb mesh coated with alumina sol and chloroplatinic acid (Park et al., 2011)
ISPC Russian Energy Technologies (Russia)	Ceramic cylindrical rod wash coated with Pt and assembled upright in a stainless-steel frame (Avdeenkov et al., 2018)
NIS (Germany)	Cartridges filled with porous ceramic spherical pellets coated with Pd (Tietsch et al., 2010)

An innovative type of PAR catalyst has been developed by the Redkino Catalyst Company (Russia) A high porosity material is made from a nickel alloy with an external ceramic layer, and coated with Pt and Pd (Bezgodov et al., 2022). Gasparyan et al. (2015) investigated a similar high-porosity ceramic material (HPCM) supported by a Pd catalyst and established that the HPCM catalyst is highly advantageous in terms of effective hydrogen catalytic oxidation (Gasparyan et al., 2015).

Although there are several possible PAR catalyst shapes and support materials, the most accepted and widely used are the plate-type catalyst (Reinecke et al., 2010) and the cylindrical-type catalyst (Kirillov, 2022).

Numerous experiments and numerical validations (ANSYS–CFX, SPARK, REKO-DIRECT) have been performed on the REKO-3 experimental facility (Jülich, Germany) to investigate the reaction kinetics of catalytic hydrogen recombination on the plate-type catalyst (cut-out of AREVA PAR FR90) (Klauck et al., 2014; Reinecke et al., 2004; Rozeń, 2015b). The catalyst is SS plates coated with a Pt/wash-coat, arranged in parallel inside the vertical channel. The gas mixture passes the catalyst section containing four catalyst plates (square surface 143 × 143 mm and thickness 1.5 mm). Experiments have been performed for different flow rates, inlet hydrogen concentrations and temperatures. The authors determined a fast start-up characteristic and nearly complete hydrogen conversion (90 %) under the considered inlet conditions. However, the surface temperature of 500 °C at the leading edge of the catalyst plates was reached during the first six minutes at $C_{in}[H_2] = 4$ vol% hydrogen exposure. It has also been mentioned that plate-type PAR catalysts can lead to the unintended ignition of hydrogen due to the overall overheating of the catalyst.

In another study by Meynet and Bentaib the experiments on a plate-type PAR catalyst were validated numerically by using SPARK code (Meynet and Bentaib, 2012). A detailed two-dimensional (2D) numerical model was developed to capture ignition criteria for the plate-type PAR catalyst and to investigate PAR operational behaviour under oxygen starvation conditions. It was found that, within the hydrogen concentration range $C_{in}[H_2] = 0$–5.4 vol%, no gas-phase combustion occurs. However, the gas-phase combustion process leads to an increased heat release rate from $C_{in}[H_2] = 5.4$ vol%. Analysis of PAR oxygen starvation demonstrates an interesting relationship between PAR efficiency and oxygen content. The numerical simulations confirmed experimental results that oxygen supply is necessary to ensure the optimal operation of a PAR. However, the ignition criteria for the plate-type catalyst was not discussed from the point of view of high catalyst temperature.

Yet another type of PAR catalyst is manufactured by ISPC Russian Energy Technologies (Moscow, Russia) (Avdeenkov et al., 2018). The catalyst is cylindrical rods made with γ-Al_2O_3, have dimensions approximately 64 mm length and 5.2 mm diameter, and assembled vertically in an SS (stainless-steel) frame. A model series of PAR has been developed, including RVK-500, RVK-1000, etc., which differ one from another in the number of catalyst sections and capacity (Keller, 2007). Initially, numerous tests were performed by the manufacturer and some authority research organisations to investigate PAR efficiency. An early study of the PAR RVK-500′s main characteristics and safety performance was conducted at the State Scientific Center of the Russian Federation Institute of Physics and Power Engineering (SSC RF-IPPE). The authors determined that the recombiner productivity was 40 %–50 % for the tested recombiner type, under the applied conditions. During the test under $C_{in}[H_2] = 5$ vol% of inlet H_2, the catalyst surface achieved a maximum surface temperature of 320 °C, which is below the lower ignition temperature of hydrogen in air (STP) (~560 °C).

In a recent experimental study by Bezgodov et al. the start-up behaviour and ignition limit of cylindrical catalyst elements was

compared to HPCM catalytic elements. The experimental series was performed in a chamber with an effective volume of 15 m^3, represented by a vertical cylinder with elliptical covers. During the experimental series, hydrogen was fed into the chamber at 60 °C, with relative humidity <5 % and 100 %, and pressure 0.1 MPa until the volume fraction of 0.5 vol% for HPCM and 1.0 vol% for the cylindrical catalyst was reached in the chamber. Results indicated similar behaviour for both types of catalyst. It was observed that the PAR commences its operation when natural convection flow is established through the channel. The ignition limit is dependent on the geometry of the catalytic elements. However, the cylindrical-type PAR catalyst needs to be studied in further detail under different initial conditions (Bezgodov et al., 2022).

3. Recent studies of cylindrical-type PAR catalyst

3.1. Experiments on the recombiner sections testing station

Extensive research has been carried out at HySA Infrastructure (North-West University, South Africa) in efforts to clarify the experimental and numerical interactions of the CHC reaction kinetics, catalyst temperature distribution, hydrogen conversion, heat, and mass transfer phenomena over the cylindrical-type catalyst PAR section. The series of tests were carried out in a small-scale test facility named the recombiner sections testing station (RSTS) at one selected (pre-determined) mass flow rate to obtain appropriate velocity distribution across a single catalyst section. Seeking to investigate the operational behaviour of a cylindrical-type catalyst under various initial conditions, and to evaluate catalyst temperature distribution and hydrogen conversion efficiency, the research was focused on a wide range of inlet hydrogen concentrations. In this context, selected parameters were measured during experiments at the in-house developed test facility.

The catalyst section is derived from the non-disclosure commercial PAR RVK-500 model, manufactured by ISPC RET (Moscow, Russia) (Avdeenkov et al., 2018). The RVK has an SS casing (vertical channel) equipped with cylindrical rods as catalytic elements. These elements are assembled upright in an SS frame. Thereafter, these frames are assembled into the catalytic block at the lower section of the PAR channel. The cylinders are made of a γ-Al_2O_3 porous ceramic base wash-coated with

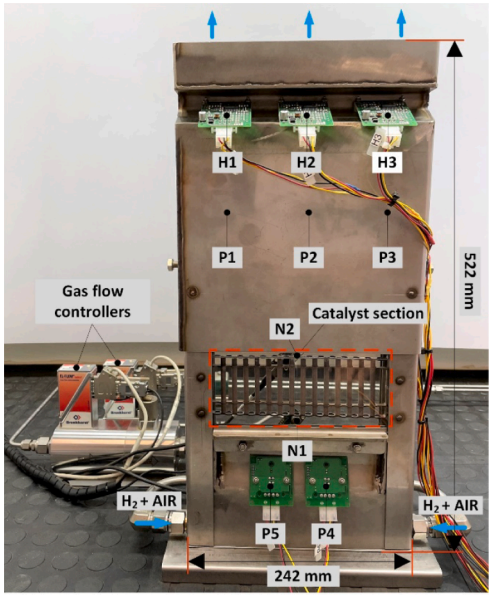

(a)

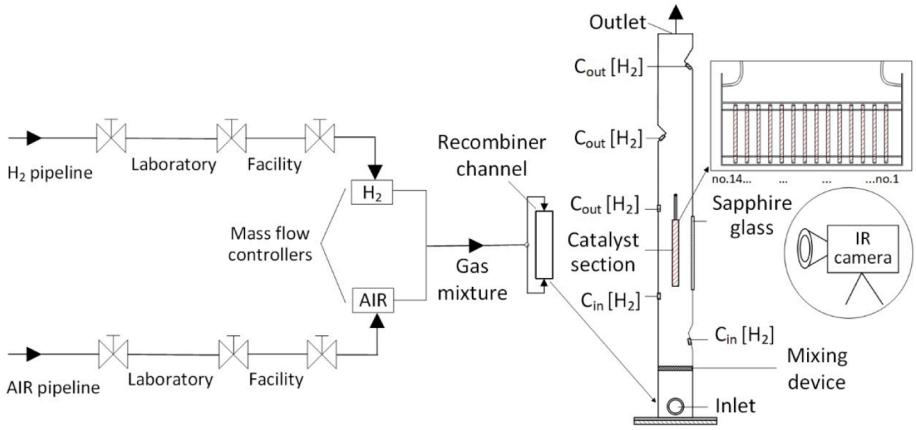

(b)

Fig. 1. RSTS facility at HySA Infrastructure, NWU: (a) general view of the channel and support infrastructure; (b) facility schematic representation.

Pt. The single cylinder is coated with a hydrophobic thin layer of polytetrafluoroethylene (pore size a few fractions of a micrometer accessible to gas) (Keller, 2007; Malakhov et al., 2020b). The dimensions of cylindrical elements are 64.0 ± 0.1 mm in height and 5.2 ± 0.1 mm in diameter.

The experiments described in this study were performed in a small-scale test facility (RSTS, HySA Infrastructure), see Fig. 1(a). It has a vertical channel with a cross-section area of 45.5 × 242 mm. The facility allows the study of a catalytic section under well-defined conditions, i.e., mass flow rate and hydrogen inlet concentration. The RSTS is equipped with digital gas flow controllers to supply the hydrogen–air mixture to the channel inlet. The application of this facility is justified by the fact that the channel represents a downscaled PAR that contains only one catalyst section. Such small-scale test facilities have long been identified as most suitable for catalytic reactions, especially in hydrogen oxidation reactions (Reinecke et al., 2004; Hunt et al., 2018; Gardner et al., 2021; Kozhukhova et al., 2022).

Fig. 1(b) presents a schematic arrangement of the experimental facility components and infrastructure, such as gas pipeline, hydrogen sensors, IR camera, and channel. Inlet and Outlet have a rectangular shape with a cross-section area of 45.5 × 242 mm. The hydrogen sensors co-called H1, H2, H3, P1, P2, P3, P4, P5 are located in the triangle slots according to Fig. 1(a).

The total inlet mass flow rate is defined to be 35.0 ± 0.2 g/min. The selected mass flow rate is appropriate to maintain the average flow velocity inside the channel. According to the CFD simulations, an average velocity along the catalyst section area was observed of <0.1 m/s. Steady-state conditions were achieved within ~600 s after initiation of a test. The initial conditions of the tests are given in Table 2.

The mixture enters the channel from the bottom, and then passes through the catalyst in the middle; steam with unreacted hydrogen exits the channel through the chimney outlet. During the experiments, the hydrogen concentration was determined in real time at 10 points inside the recombiner channel. The sensors manufactured by Neodym ProtiSen (P and H) and Xensor Integration XEN-5320 (N) were used in the experiments. P and H were used to calculate the average H_2 concentration when N sensors – for the local concentrations. ProtiSen sensors detect hydrogen (in the air) with a range of 0–4 vol%. XEN-5320 sensors detect hydrogen with a range of 0–100 vol%. The inlet hydrogen concentration was measured at two lowest points of the channel by ProtiSen sensors (P4, P5) and one local point near the catalyst section by XEN-5320 sensors (N1). The outlet hydrogen concentrations (average) were measured at six upper points along the channel by ProtiSen sensors (P1, P2, P3, H1, H2, H3), and one local point near the catalyst section by XEN-5320 sensors (point N2). The measuring error of hydrogen concentration did not exceed ±3 %.

The initial temperature of the catalyst was in the range 25–28 °C. The temperature distribution over the catalyst surface was captured with a high-resolution infrared (IR) camera (Telops Midwave HD Series (M100hd), Canada). Base calibration of accuracy and uniformity were performed by Telops and the absolute error was estimated within ±2 °C for the temperature range 0–345 °C, and ±4 °C for the temperature range 345–600 °C. Thermal and optical visibility was achieved by equipping the facility channel with sapphire glass placed in front of the catalyst section.

Some representative results are given in Figs. 2–7. They demonstrate the constant inlet H_2 concentration (black line), local (red line), and average (blue line) outlet H_2 concentration, and the evolution of catalyst surface temperature (green line). The local outlet hydrogen concentration curve represents the N2 sensor reading, while the average outlet hydrogen concentration curve is an average value out of the six upper sensor readings (P1, P2, P3, H1, H2, H3). The catalyst surface temperature increases due to the exothermic recombination reaction, depending on hydrogen concentration. The green lines in Figs. 2–7 illustrate this effect.

Table 2
Initial conditions of the test series.

H_2 inlet concentration $C_{in}[H_2]$, vol.%	Mass flow rate $\dot{m}_{in}$, g/min	P_0, kPa	T_{0gas}, °C
2.0–7.0	35.0 ± 0.2	101	25

It is evident from these figures that the maximum catalyst surface temperature (T_{max}) increases as the inlet hydrogen concentration increases. The maximum temperature at 2 vol% hydrogen concentration reaches nearly 180 °C, while the highest temperature of approximately 405 °C at 7 vol% of inlet H_2 is observed. Fig. 3 shows that T_{max} reaches 235 °C at 3 vol% inlet H_2. Under conditions that refer to the lower hydrogen ignition limit (4 vol%), T_{max} reaches ~275 °C (Fig. 4). The maximum temperature at 5 vol% and 6 vol% inlet H_2 reaches 310 °C and 365 °C, respectively (Figs. 5 and 6). Nevertheless, the minimum hydrogen ignition temperature in atmospheric air (about 540–580 °C) (Avdeenkov et al., 2018; duToit et al., 2018; Kozhukhova et al., 2021b) was not observed under the given experimental conditions. The experimental results obtained for the catalyst temperature demonstrated a safe and reliable performance of the cylindrical-type PAR catalyst within a wide range of inlet hydrogen concentrations.

On the other hand, it is interesting to observe the time duration required for the catalyst to achieve steady-state conditions under different inlet hydrogen concentrations. Fig. 2 reveals that the catalyst temperature keeps rising, within approximately 400 s, before it reaches the maximum value. However, this trend changes slightly as the hydrogen concentration increases. For the remainder of the given cases, the catalyst reaches T_{max} after nearly 250 s of hydrogen exposure.

Regarding the temperature gradient along the horizontal axis of the catalyst section, it is necessary to explain the difference in the surface temperature profiles obtained from experiments. Based on the full 2D profiles obtained from the IR camera, a significant temperature gradient was observed between cylinder no.1 and cylinder no.14. Fig. 8 demonstrates this phenomenon. The initial conditions for Test 1 and Test 2, described here were identical to those of the main test series outlined in Table 2, for $C_{in}[H_2] = 7$ vol%. At high hydrogen concentrations, some instability in the horizontal temperature gradient may appear. The experimental channel has an open top part (exhaust), and the outgoing flow rates are low. Therefore, any reasons causing a violation of the installation's insulation can lead to a redistribution of gas flows both near the setpoint and in it. This in turn causes flow asymmetry in the experiment and a corresponding horizontal temperature gradient. Our goal was to achieve as symmetrical temperature distribution as possible and in the latest experiments, we observed a relatively symmetrical temperature profile along the horizontal axis of the catalyst section under the entire range of hydrogen concentration.

According to the above, we have a ground to consider that there are two similar flow behaviours observed during the cylindrical-type catalyst operation, specifically, either the translocation of the gas mixture at the right/left or the symmetrical flow over the middle part of the catalyst section/recombiner channel. We note that the catalyst temperature demonstrates a very similar maximum for both observed flow behaviour. This conclusion is reinforced by CFD simulations (see Section 3.2).

Besides the catalyst temperature, the hydrogen conversion rate is the most significant parameter of PAR operation. Figs. 2–7 (blue line) present the time evolution of the average hydrogen concentration at the outlet of the recombiner channel. These hydrogen concentrations were obtained for all cases considered in this study (2–7 vol%) at an inlet gas temperature of 25 °C and a mass flow rate of 35.0 ± 0.2 g/min.

The initial phase of hydrogen consumption is observed during the first 30 s. Although the hydrogen concentration at the outlet increases over the first 30 s, it never reaches the inlet concentration. This increase in concentration can be referred to the low temperature of the catalyst section, which was within the range 26–30 °C. Then, after 30 s, the hydrogen concentration decreases, which means that the autocatalytic recombination reaction has commenced. The hydrogen concentration

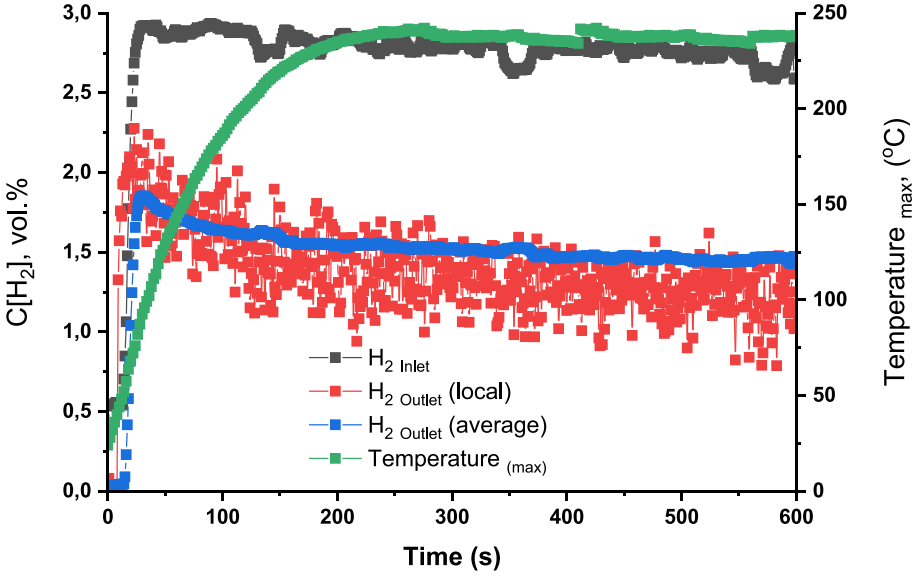

Fig. 2. Time evolution of catalyst surface temperature and outlet H_2 concentrations at $C_{in}[H_2] = 2$ vol%.

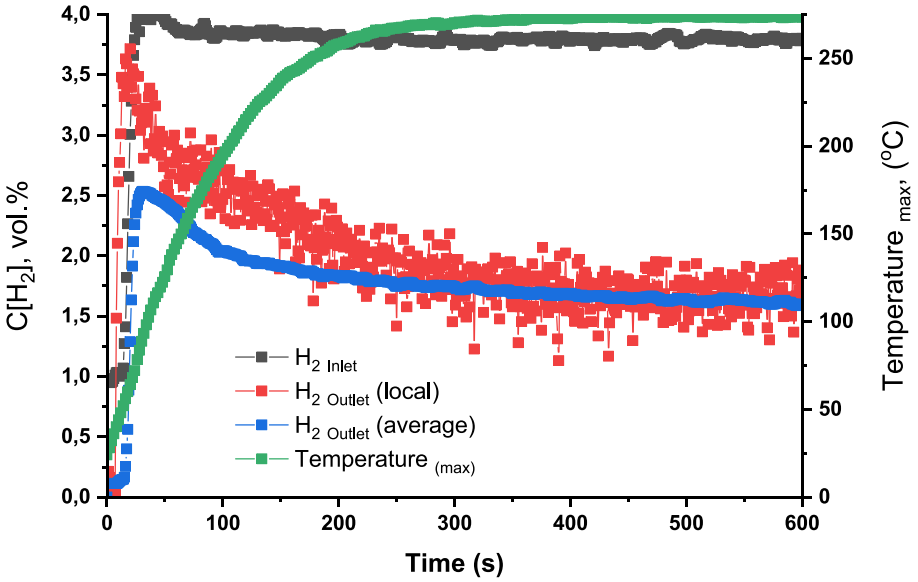

Fig. 3. Time evolution of catalyst surface temperature and outlet H_2 concentrations at $C_{in}[H_2] = 3$ vol%.

continues to decrease up to 120 s. A relatively uniform outlet hydrogen concentration can be observed within 300 s of recombiner operation. The steady-state concentration at the channel outlet was achieved after ~ 600 s of hydrogen exposure. Similar results of PAR start-up behaviour for the plate-type PAR catalyst were observed by Rożeń (2018). Experiments with both catalyst types, generally, demonstrated that the recombination reaction occurs spontaneously on the catalyst surface.

The hydrogen conversion rate is influenced by a wide range of factors, including but not limited to the inlet flow rate, hydrogen concentration, relative humidity, gas temperature, the presence of carbon monoxide and the gas residence time on the catalyst surface (Gupta et al., 2015; Mueller et al., 1999; Reinecke et al., 2004; Malakhov et al., 2020b; Kozhukhova et al., 2021a; Malakhov et al., 2022). The latter parameter can be ascribed to the PAR's channel design and the shape of catalytic elements. The results demonstrate that hydrogen recombination in the recombiner channel is incomplete. The reaction products and unreacted hydrogen passes through the gas outlet. Therefore, the hydrogen conversion (Y_{H2}, %) can be quantified by Eq. (1):

$$Y_{H2} = \frac{C_{in[H2]} - C_{out[H2]}}{C_{in[H2]}} \times 100 \quad (1)$$

with the use of measured outlet and inlet hydrogen concentrations.

It is well known that hydrogen conversion increases with an increase in inlet hydrogen concentration (Reinecke et al., 2014). From the results obtained in the RSTS experiments, the cylindrical-type catalyst section demonstrates similar behaviour. Based on the data presented in Table 3, the lowest conversion efficiency of ~50 % was observed at $C_{in}[H_2] = 2$ vol%, while the highest efficiency of 67 % was observed at $C_{in}[H_2] = 7$ vol%. Experimental conversion efficiency is estimated within the range 50 %–68 %. Avdeenkov et al. have reported almost identical experimental results for the same cylindrical-type PAR catalyst (Avdeenkov et al., 2018). Besides that, results for both catalysts demonstrated that >50 % of incoming hydrogen is converted into water and heat within all the hydrogen concentrations considered.

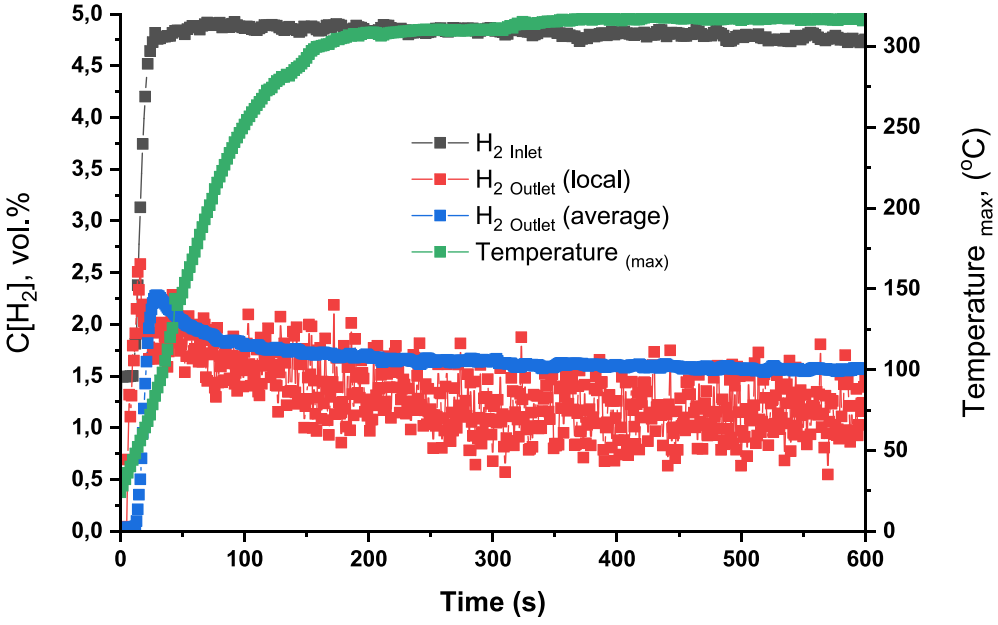

Fig. 4. Time evolution of catalyst surface temperature and outlet H_2 concentrations at $C_{in}[H_2] = 4$ vol%.

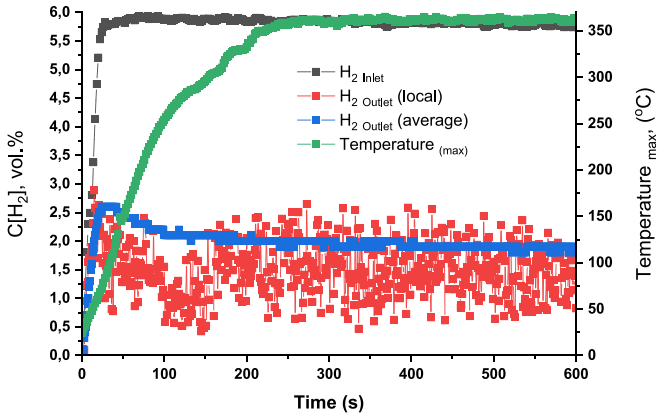

Fig. 5. Time evolution of catalyst surface temperature and outlet H_2 concentrations at $C_{in}[H_2] = 5$ vol%.

3.2. Detailed CFD modelling in STAR-CCM+

The test model described in the experimental section (Section 3.1) was validated in CFD code STAR-CCM+ (Siemens PLM Software, U.S.) in combination with the CHEMKIN database (Reaction Design, U.S.). A 3D detailed CFD model was designed to represent the same vertical channel with a cross-section area of 242.0 × 45.5 mm, containing a single cylindrical-type catalyst section. The flow inside of the channel is assumed turbulent due to the complex geometry of the catalyst section. In the present study, the choice of the realisable k-ε model over the LES turbulence model or others is motivated by practical considerations. The LES model is computationally more efficient for some simulation cases; however, it requires higher computational resources and longer CPU wall time. A realisable k-ε model has several advantages over other turbulence models, such as k-ω SST. A realisable k-ε model is well-suited for capturing the averaged behaviour of turbulent flows, which is often sufficient for many engineering applications. The realizable k-e model turbulence viscosity is not a constant like in the standard model but a variable. Since velocity keeps on changing its vector throughout the channel, the realizable k-e model is more suitable for simulations of the near-wall vortices. Therefore, a realisable k-epsilon model with a two-layer approach based on Reynolds-averaged Navier–Stokes equations was used to simulate turbulent flow (Malakhov et al., 2020a).

The standard mesh sensitivity study was performed using three base mesh sizes of 10.0 mm, 5.0 mm, and 1.0 mm. Mesh refinement was applied around the catalyst section area for all base cell sizes. The results indicated that the numerical solutions were insensitive with 5.0 mm of base cell size. Polyhedral-type mesh with a total number of ~3,500,000 cells is discretised in the numerical domain. Numerical mesh settings and boundary conditions are presented in Fig. 9.

A preliminary numerical study of cylindrical-type PAR catalyst characteristics within the inlet hydrogen concentration range 2–5 vol% was performed by Malakhov et al. (2020b). Based on the assumption that the study conditions lie below those for a possible occurrence of homogeneous combustion, only a heterogeneous mechanism of H_2/O_2 recombination on Pt catalyst was included in the numerical model (Deutschmann et al., 1996).

However, to study the catalytic hydrogen recombination process in detail, one has to keep in mind that it is necessary, to take into account the homogeneous reaction kinetics mechanism in the CFD model (Klauck et al., 2014). The numerical model which includes surface and gas-phase reaction kinetics was introduced and validated by several authors (Appel et al., 2002; Deutschmann et al., 1996; Ljungström et al., 1989; Mueller et al., 1999; Rinnemo et al., 1997; Warnatz et al., 1994; Zhang et al., 2020).

In efforts to investigate a cylindrical-type PAR catalyst under a high inlet hydrogen concentration, a detailed CFD model that includes the conjugated approach of H_2/O_2 recombination reaction kinetics has been proposed in recent work by Malakhov et al. (Malakhov et al., 2022) based on works published in past (Appel et al., 2002; Klauck et al., 2014). The detailed mechanism contains twelve heterogeneous and twenty-one homogeneous chemical reactions (Deutschmann et al., 1996; Warnatz et al., 1994).

The reaction rate results from the sum of reaction rates of each surface and gas-phase species obtained from the detailed chemical mechanism of hydrogen oxidation on a Pt catalyst (Appel et al., 2002). The reaction rate coefficient for reaction *j* is calculated by the Arrhenius equation as shown in Eq. (2):

$$k_j = AT^{\beta}\exp\left(-\frac{E_a}{R_u T}\right) \tag{2}$$

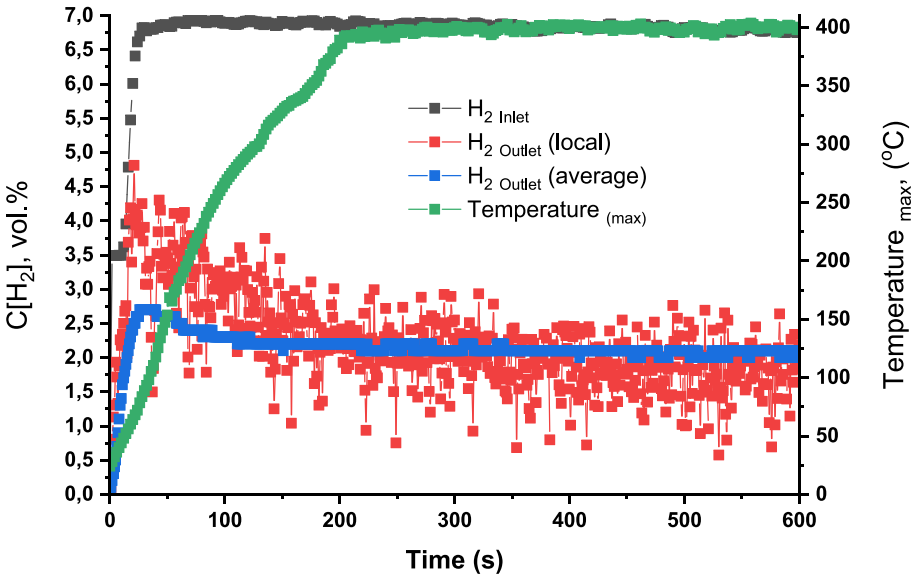

Fig. 6. Time evolution of catalyst surface temperature and outlet H_2 concentrations at $C_{in}[H_2] = 6$ vol%.

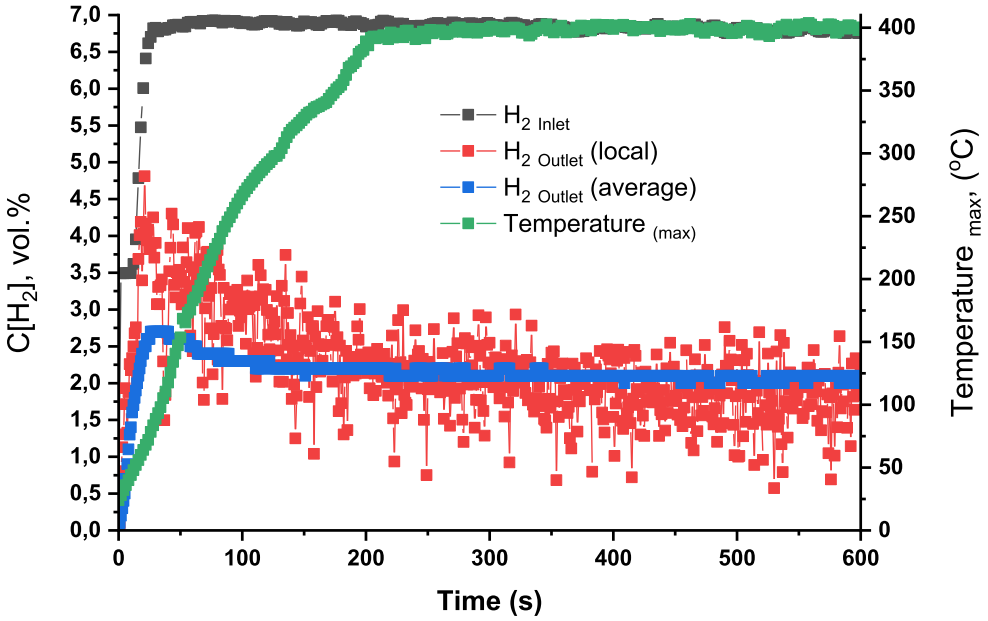

Fig. 7. Time evolution of catalyst surface temperature and outlet H_2 concentrations at $C_{in}[H_2] = 7$ vol%.

where R_u is the universal gas constant and A is the pre-exponential coefficient, E_a is the activation energy and β is the temperature coefficient that is supplied by the chemical mechanism (Appel et al., 2002; Klauck et al., 2014; Rinnemo et al., 1997). The surface mechanism comprises 12 reactions—hence it can provide absorption–desorption reactions of the gas species on the catalyst and surface species for surface reactions. The results demonstrate that hydrogen recombination reaction occurs in the diffusion regime (Frank-Kameneckij, 1955). In this case, the amount of Pt loaded does not play a significant role in the reaction rate and the main rate-controlling process is the gas diffusion to the surface (Prabhudharwadkar et al., 2011; Rozeń, 2018). Therefore, the cylinders supported by the Pt catalyst were simulated as a smooth Pt layer with the surface site density taken as 2.7×10^{-8} kmol/m^2. Thermochemical properties were taken from the CHEMKIN thermodynamic database and applied with polynomial curves (Ljungström et al., 1989; Mantzaras et al., 2009; Meynet et al., 2014).

Heat radiation generated from catalytic elements as a result of exothermal reaction is an important component of heat transfer inside a PAR (Rozeń, 2015a). According to Meynet et al., thermal radiation and thermal diffusion modelling have a significant effect on the numerical results (Meynet et al., 2014). The difference in temperature prediction, caused by radiation model presence was also observed in the proposed CFD model, however, not present in this work. Considering the literature, heat radiation from the catalyst surface is accounted for by using the discrete ordinates method (DOM). Catalyst surface emissivity was set to a value of 0.9 for platinum black (Rozeń, 2015b). The definition of transport of mass was accomplished by including the multicomponent diffusion of each species involved in the gas mixture. Furthermore, recent numerical studies have demonstrated that the mass transfer caused by the thermal diffusion effects on prediction of catalyst temperature and hydrogen distribution in a PAR channel (Rozeń, 2015a,b; Malakhov et al., 2023). In the final step, an additional equation that accounts for the thermal diffusion (Soret effect) was added to the

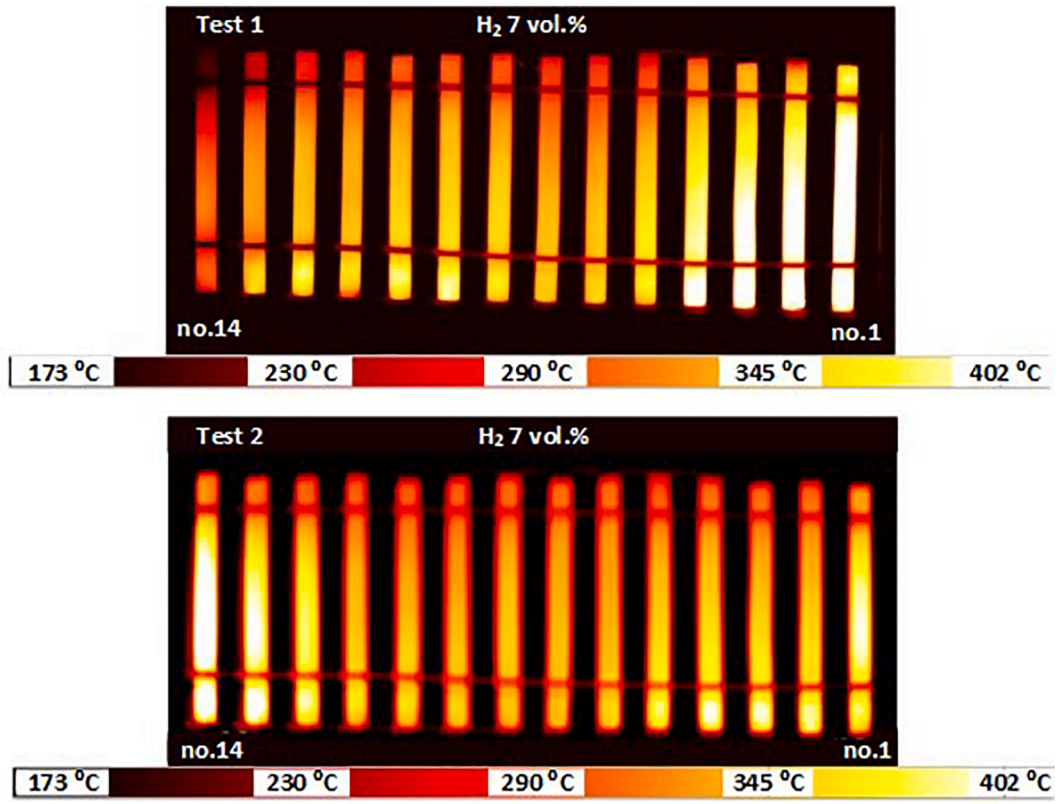

Fig. 8. Comparison of experimental temperature profiles obtained with an IR camera at $C_{in}[H_2]$ = 7 vol%.

Table 3
Experimental hydrogen outlet concentrations and estimated conversion.

H_2 inlet concentration $C_{in}[H_2]$, vol.%	H_2 outlet concentration $C_{in}[H_2]$, vol.%	H_2 conversion, %
2.0	1.05	47.5
3.0	1.46	51.4
4.0	1.75	56.25
5.0	1.9	62.0
6.0	2.1	65.0
7.0	2.26	67.7

detailed CFD model. For a more detailed description, the reader is referred to literature (Malakhov et al., 2023).

It is worth noticing that the CFD simulations included all fourteen catalytic cylinders and full-length channel as shown in Fig. 9. The full-scale profiles can be found in supplementary materials. Fig. 10 presents an example of the calculated distribution profiles of flow velocity, temperature, reactants, and products along two cylinders in the middle of the recombiner channel (cylinders no.7 and no.8) at 5 vol% hydrogen. Results demonstrate steady-state calculations.

Although the mass flow rate at the inlet pipe of the recombiner channel is relatively high (0.29167 g/s for each inlet side in the CFD model (see Fig. 1)), the flow at the lower part of the channel demonstrates 0.1–0.2 m/s. Moreover, a low-velocity profile of <0.1 m/s was observed along the catalyst section area, as can be seen in Fig. 10(a).

Simulation results demonstrated that, due to assumed symmetry in the CFD model, the temperature distribution shows a similar pattern for all cases studied in this paper, i.e. the maximum temperature is found along the middle cylinders. It should be noted that the experimental temperature profiles reveal the hottest cylinders on the very right or left side of the catalyst section, however, the maximum value stays the same, regardless of the place it appears. It can be attributed to the specifics of turbulent vortex distribution in the experimental channel. Fig. 10(b) shows the catalyst surface temperature at 5 vol% inlet H_2 for the 7th and 8th cylinders (in the middle of the catalyst section) that reaches 310 °C. The simulation results demonstrate an excellent prediction of the experimentally measured maximum temperature. Our preliminary results demonstrated that the effect of homogeneous mechanism is rather small for up to 7 % of inlet H_2 but detailed analysis and effects will be studied elsewhere. The observed deviation between measured and calculated maximum catalyst surface temperature observed in the present study did not exceed 5 % (see Fig. 11) while it can be more for some arbitrary locations.

Fig. 10(c) shows that the hydrogen concentration over the catalyst elements is nearly zero, which means that hydrogen recombination occurs rapidly on the catalyst surface. In the considered case, the velocity along the cylinders is quite low (Fig. 10(a)), and it can be concluded that the recombination reaction occurs in the diffusion regime. Moreover, Fig. 10(c) demonstrates an interesting phenomenon. In the case of a cylindrical-type catalyst, the SS frame, which holds the cylinders together, absorbs heat radiated from the catalyst. As a result of the separation of the light and heavy reaction species, there is an accumulation (in concentration) of light hydrogen species near the SS frame at the bottom of the middle group of catalyst cylinders (where the temperature gradient is higher). This can be attributed to the difference in thermal conductivity of the catalyst support material and the SS frame. Therefore, the temperature gradient between the heated catalyst and surrounding gas causes the local hydrogen concentration near the SS frame to increase due to thermal diffusion. Simulations demonstrated that the value of the thermal diffusion effect (Soret effect) increases as the inlet concentration increases (Malakhov et al., 2023).

It is evident that water vapour is gradually generated during the H_2/O_2 reaction and then transports up the channel exit by convection. Fig. 10(d) illustrates the profile of H_2O distribution. According to our simulations, the amount of H_2O close to the catalyst surface reaches 12 vol% at 5 vol% of inlet H_2. In a study of plate-type catalyst behaviour under carbon monoxide poisoning conditions, Klauck et al. reported 8 vol% of outlet H_2O at 5 vol% of inlet H_2 (Klauck et al., 2014).

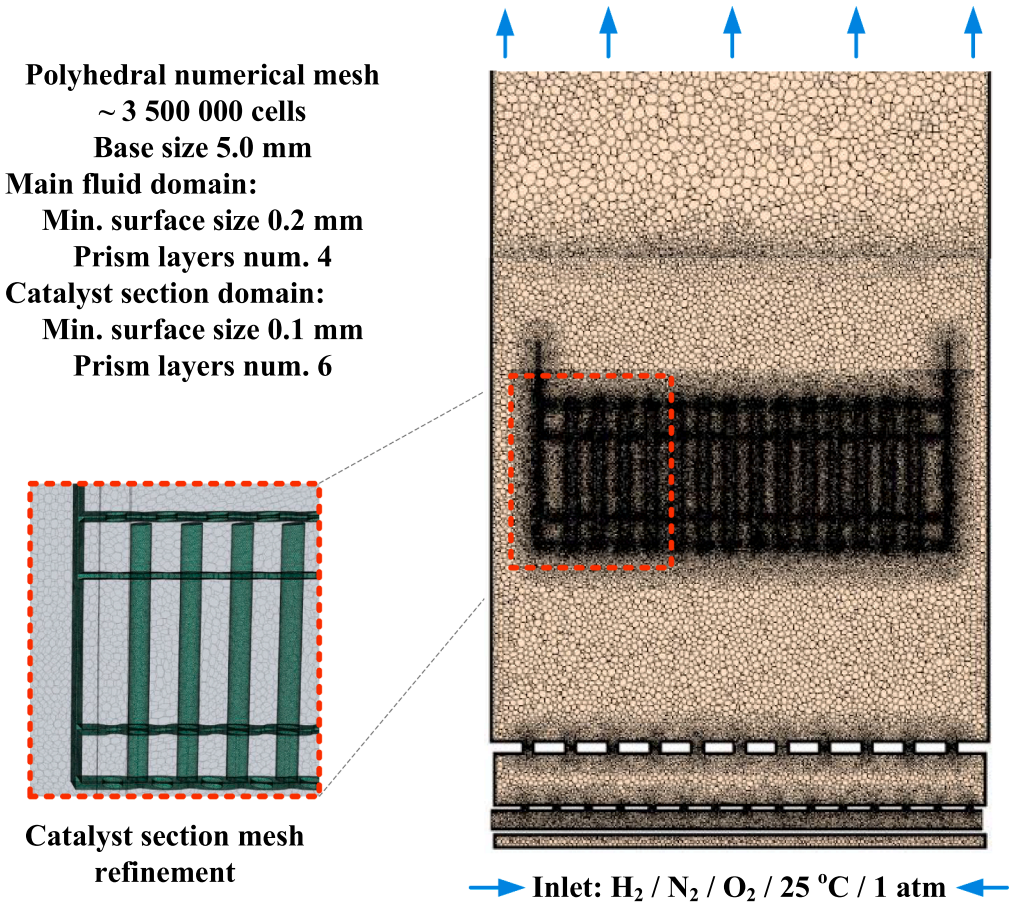

Fig. 9. Catalyst section mesh refinement and general view of numerical mesh.

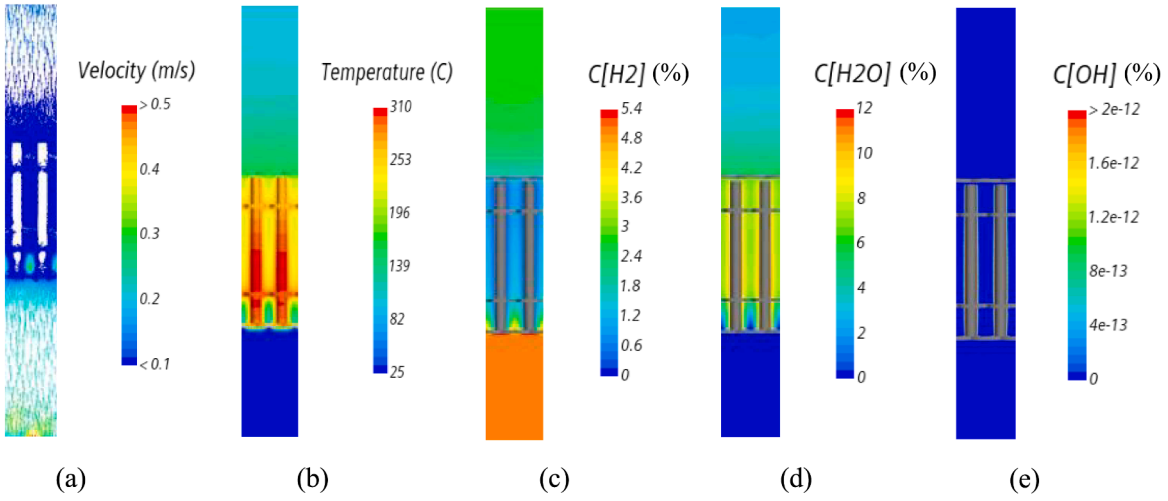

Fig. 10. Numerically calculated profiles at $C_{in}[H_2] = 5$ vol% (a) flow velocity, (b) catalyst surface temperature, (c) H_2 concentration, (d) H_2O concentration, (e) OH concentration.

Fig. 10(e) presents the OH– radical mole fraction profile along the middle of the catalyst section. The concentration of OH– radicals in reaction products can be an indicator of hydrogen ignition occurring in the gas phase (Dogwiler et al., 1999; Ljungström et al., 1989). In a plate-type catalyst study, Meynet et al. demonstrated the availability of OH– radicals with a maximum 1.0×10^{-3} mole fraction of OH– at 8 vol% of inlet H_2 (Meynet et al., 2014). However, in the present paper, the numerically calculated outlet mole fraction of OH– does not exceed 2.0 $\times 10^{-12}$ at 5 vol% of inlet H_2.

A comparison of the maximum catalyst temperature measured experimentally over the cylindrical-type catalyst section against CFD simulation is presented in Fig. 11. The maximum temperature is calculated for all 14 cylinders and the hottest catalyst cylinder is plotted along the ordinate axis, while the cylinder length is plotted along the abscissa axis (0.065 m is the lower part (bottom), 0.0 m is the upper part (top) of catalyst cylinders).

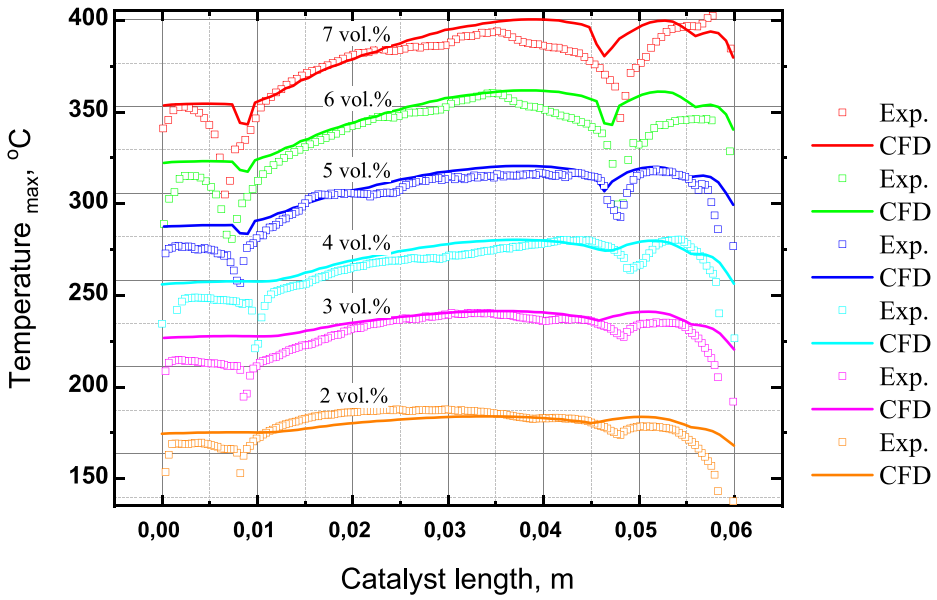

Fig. 11. Numerical and experiment temperature profiles at $C_{in}[H_2]$ = 2–7 vol%.

The catalyst temperature profiles are predicted reasonably well by the CFD model. The catalyst temperature profiles demonstrate a fairly homogeneous distribution along the cylinder length; the temperature difference between the upper and lower parts does not exceed 10 °C at $C_{in}[H_2]$ = 2 vol%. However, the temperature gradient increases as the inlet hydrogen concentration increases, until it reaches ~Δ 50 °C at $C_{in}[H_2]$ = 7 vol%. Results demonstrate that the majority of hydrogen reacts on a lower part of the catalyst section, which reflects in a higher maximum temperature on that part of the catalyst. Maximum temperature of ~405 °C for the catalyst surface is observed at $C_{in}[H_2]$ = 7 vol%. Considering the minimum ignition temperature for hydrogen at STP of ~560 °C, the cylindrical-type PAR catalyst has not reached an ignition temperature, even under the highest concentration considered in the current study.

It can be seen that minimum temperatures at the very top and bottom points of catalytic cylinders (0.0 m and 0.065 m) present different values in the experiment and simulations. It can be attributed to the fact that the experimental temperature was taken on the SS frame that holds the cylinders upright, instead of the actual catalyst temperature. The two humps of the temperature drop can be attributed to the SS frame that holds the catalytic cylinders upright. Due to the geometrical features, the frame absorbs radiative heat from the catalyst surface at two points, as can be seen in Fig. 11. The difference between the numerical and experimental results increases as the H_2 concentration increases. Nevertheless, although the average maximum catalyst temperature gets overpredicted as the initial hydrogen concentration increases, it can be confirmed that global characteristics of the catalyst surface temperature profile can be reproduced in good agreement with experimental data.

Fig. 12 shows experimentally measured and CFD simulated steady-state hydrogen conversion. As mentioned in Section 3.1, conversion increases as the inlet hydrogen concentration increases. The lowest efficiency of ~ 50 % was observed at $C_{in}[H_2]$ = 2 vol%, whilst the highest efficiency of 65 % was observed at $C_{in}[H_2]$ = 7 vol%.

Numerically calculated hydrogen conversion shows a difference. Fig. 12 shows that the calculated hydrogen conversion increases as the inlet hydrogen increases from 2 vol% to 7 vol%. It can be seen that the discrepancy of the results increases when inlet hydrogen concentration increases. The relative error between experimental and simulation for hydrogen conversion is about 10 %. The hypothesis is that due to the transition between surface and gas phase chemistry from $C_{in}[H_2]$ = 5 vol % the discrepancy between the experiment and CFD increases. It was

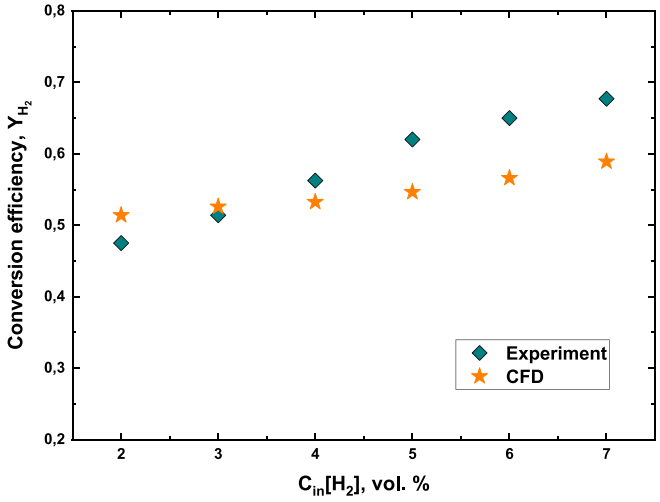

Fig. 12. Numerical and experimental hydrogen conversion at $C_{in}[H_2]$ = 2–7 vol%.

found that, for instance, AREVA PAR starts gas phase recombination at around $C_{in}[H_2]$ = 6 vol% (Meynet and Bentaib, 2012). Consequently, from around $C_{in}[H_2]$ = 6 % the gas phase reaction contributes more to the hydrogen recombination process in PAR. For the cylindrical PAR catalyst, the gas phase ignition limit will be investigated in future work.

From the hydrogen conversion point of view, the plate-type catalyst demonstrates significantly higher efficiency than the cylindrical-type (Klauck et al., 2014). However, when making comparisons, one should take into account the following: the channel geometry of the REKO (Germany) and RSTS (South Africa) facilities and the total area of catalyst surfaces.

3.2.1. *Specific issue: modelling of turbulent mass transport*

CFD simulation of turbulent flow dispersion is generally performed using Reynolds-Averaged Navier–Stokes (RANS) or Large-Eddy Simulation (LES) turbulence models. An important issue related to turbulence flow modelling is how to choose the turbulent Schmidt number (Sc_t). The Schmidt number is the ratio of the kinematic viscosity and the molecular diffusivity (Reynolds, 1975).

A wide range of predicting Sc_t values exists for different applications. According to a review by Tominaga and Stathopoulos, the optimal values of Sc_t might vary significantly, from 0.2 to 1.3 (Tominaga and Stathopoulos, 2007). The Schmidt number can be calculated through a series of CFD validations against experimental data with varying Sc_t values (Blocken et al., 2008). However, from the literature, it appears that the choice of Sc_t is not straightforward—the actual value depends on the flow properties and channel geometry. For example, Orszulik et al. performed CFD simulations in the ANSYS Fluent code and proposed that the Schmidt number equal to 1.3 allows for the best predictions in the case of plate-type PAR catalyst (AREVA FR90) (Orszulik et al., 2015). A high Sc_t number can be attributed to a likelihood of laminar flow when the low Sc_t number is linked to well-developed turbulent flow.

In STAR-CCM+, the Schmidt number is a function of molecular diffusion, therefore, when changing the Schmidt number, one changes the molecular diffusion by means Sc_t. The turbulent Schmidt number is a non-dimensional parameter that is defined by Eq. (3):

$$Sc_t = \frac{v}{D_{im}} \tag{3}$$

where, v is the kinematic viscosity and D_{im} is the molecular diffusion of component i in the mixture (CD-Adapco, 2020).

Taking the above into consideration, additional simulations were performed in this study in order to evaluate the Schmidt number influence on the catalyst temperature of a cylindrical-type PAR catalyst. The simulations were performed with the Sc_t values ranging from 0.2 to 1.0 (e.g., Sc_t = 0.2; 0.28; 0.4; 1.0) and compared to simulations with use of kinetics theory model and experiment.

Fig. 13 shows the comparison of catalyst maximum temperatures with use of different Sc_t values and kinetics theory for turbulence mass transport modelling against experimental data. In order to calculate maximum catalyst surface temperature in CFD simulation, the vertical line-probe that contains 40 trace points have been created along each catalytic cylinder attached to the surface.

For the cylindrical-type PAR catalyst it can be seen that a better prediction was obtained with use of the kinetics theory model. However, the results demonstrate that low Sc_t indicates an efficient mixing of hydrogen and air along the catalyst section, leading to a higher likelihood of turbulent flow occurring. Research has shown that Sc_t values within the range 0.2–0.28 allow for the best prediction of experimental temperature profiles under the considered conditions, as well as it shows that Sc_t number strongly correlated with hydrogen concentration.

3.3. Estimation of PAR efficiency based on mechanistic transport approach and detailed mechanism of H_2/O_2 recombination

The PAR conversion efficiency—the amount of hydrogen converted on the catalyst surface during recombiner operation—can be either measured experimentally or calculated numerically. Several research works have studied the commercially available PARs, in order to develop a simplified equation that predicts global behaviour of a PAR—the so-called empirical rate correlations was developed (Avdeenkov et al., 2018; Kelm et al., 2008; Reinecke et al., 2010). However, those works are based on empirical correlations and allow predictions of specific conditions that have been assumed in related experiments. Besides that, there is yet another method to access the practical estimation of the PAR RVK-500 conversion efficiency. Previously published works stated that the rate of recombination reaction is governed by the speed of supply of the reactants to the catalyst surface, e.g. fast surface reaction hypothesis (Kelm et al., 2008; Reinecke et al., 2010; Avdeenkov et al., 2018, 2022; Malakhov et al., 2020). This assumption can be applied to develop a numerical estimation of the entire PAR efficiency. The efficiency of the entire PAR can be estimated by using the Sherwood equation (Kelm et al., 2008).

As the PAR catalytic unit comprises numerous geometrically identical elements, it is often unnecessary to calculate the characteristics of each individual plate or rod or even the entire PAR. Instead, it suffices to examine and validate the efficiency of the smallest representative structure. This approach was employed in verifying the REKO-3 experiments (Reinecke et al., 2005). In this context, the proposed approach needs to add an additional definition of the “elementary cell” of a PAR (single section of RVK-500 catalyst). It represents the essential functional component of the system, allowing for the evaluation of the entire PAR effectiveness. For a more detailed description of the method, the reader is referred to Avdeenkov et al. (Avdeenkov et al., 2022).

The proposed method is based on two assumptions: (i) the gas mixture is considered a mixture of ideal gas and (ii) mass transport occurs in the diffusion regime (continuous plug flow reactor) (Rozeń, 2015a). For the conditions of the catalytic hydrogen recombination process occurring in the diffusion regime, the reaction rate can be approximated using the mechanistic transport approach, as follows (4):

$$R = Sh\frac{D}{d}\Delta C_M \tag{4}$$

where, Sh is the Sherwood number, D is the effective diffusion coefficient, d is the hydraulic diameter, and ΔC_M is the mole concentration of H_2.

Accordingly, in the case of the diffusion regime of hydrogen recombination reaction, Eq. (4) can be converted as follows (5):

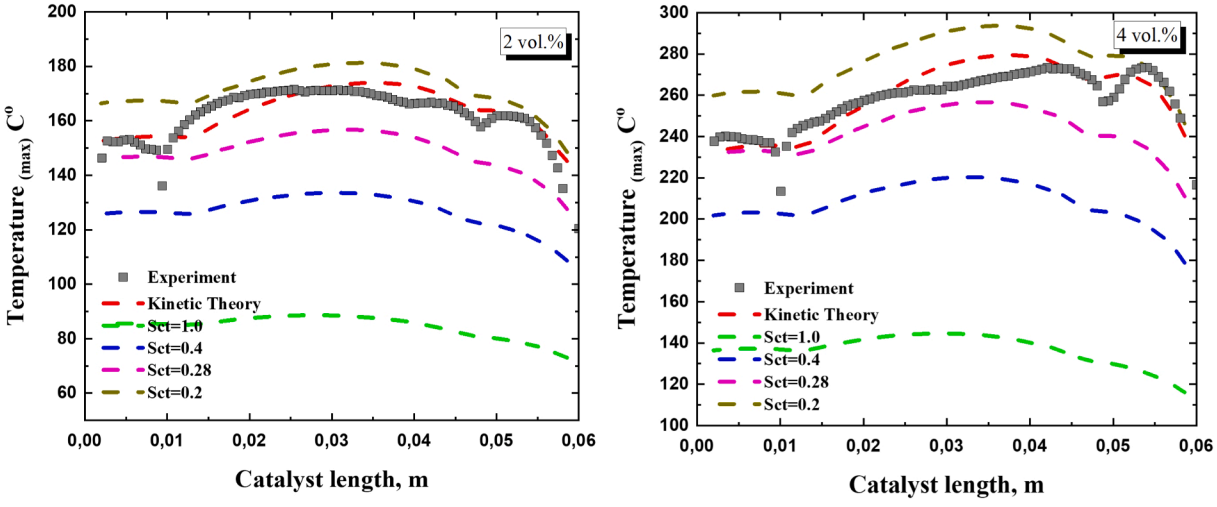

Fig. 13. Maximum temperature profile along catalytic cylinders for different Sc_t number value, kinetic theory model, and experiments at 2 and 4 vol% hydrogen.

$$R = Sh\frac{D}{d}C_M \tag{5}$$

where, C_M is the mole concentration of inlet hydrogen.

For the uniform well-developed turbulence flow, the Sherwood number can be transformed as follows (6):

$$Sh = f(Re, Sc_t) = const Re^n Sc_t^m \tag{6}$$

where, $Re = \rho w d/\eta$ is the Reynolds, $Sc_t = \eta/(\rho D)$ is the Schmidt number, η – is the dynamic viscosity and ρ is the density of the hydrogen-air mixture.

Considering that the hydrogen-air mixture is the mixture of ideal gases it is easy to see that the density is proportional to C_M/C, where C is the hydrogen volume concentration.

Thus, according to Eqs. (5) and (6) the recombination reaction rate can be rewritten as follows (7):

$$R = AC_M^{n-m}C^{m-n+1}w^n \tag{7}$$

where, A is the constant that accounts for the environmental conditions (such as pressure, temperature, mass flow rate) and channel geometry, C_M is the hydrogen molar concentration, C is the hydrogen volume concentration, and w is the flow rate.

We presumed that all coefficients for Eq. (7) can be found for the recombiner elementary cell by calculation of recombination rate for different initial conditions. The elementary cell of the recombiner is built based on the symmetry of the arrangement of the cylinders in the catalytic block and symmetrical boundary conditions. Knowing the productivity of the unit cell and their number, the overall productivity of the recombiner is simply scaled by multiplying the productivity of the unit cell by their number. Of course, this does not consider edge effects, that is, the effect of the finiteness of the catalytic unit. However, the estimation showed that for a catalytic unit containing several hundred catalytic cylinders, this effect is insignificant.

All numerical data for recombination rate of the elementary cell and for different C_M, C and w are calculated with use of a detailed mechanism in a way it was verified in previous chapters. We found that all collected data can be approximated by the following functional dependence (8):

$$R = 9.29 \times 10^{-6}(C_M C w)^{0.564} \tag{8}$$

PAR RVK-500 consists of 245 elementary cells, then the functional dependence (8) needs to be multiplied by the total number of elementary cells (Avdeenkov et al., 2022). This formula is more appropriate for the numerical investigation of recombiners. But as we are dealing with ideal gases, we can use any two other thermodynamic variables for the environmental condition instead of C_M, C, for example, P and C or T and C. Therefore, the efficiency of hydrogen recombination for the entire cylindrical-type PAR RVK-500 can be estimated for given external conditions such as temperature, pressure, flow rate and volume concentration.

In order to verify the mechanistic transport approach and functional dependence (8), some experimental data for PAR RVK-500 was taken from Tarasov et al. and Avdeenkov et al. That data was collected in the facility that ensures natural convection flow throughout the PAR channel. The flow rate was estimated within the range of 0.3–0.5 m/s. That data were used to compare results obtained by (8) against the empirical rate correlation published in the past (Tarasov et al., 2017; Avdeenkov et al., 2018).

Fig. 14 demonstrates the numerically calculated efficiency of PAR RVK-500 by functional dependence (8) under different initial conditions. The trend on Fig. 14 demonstrates that the PAR efficiency is linearly increasing as inlet hydrogen concentration increases. Furthermore, presented estimation correlates with the previously published results by (Avdeenkov et al., 2022), (Malakhov et al., 2023), (Tarasov et al., 2017).

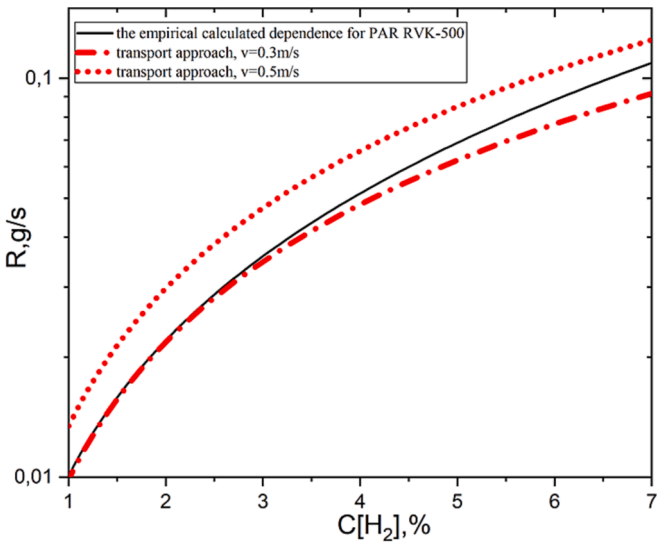

Fig. 14. PAR RVK-500 conversion efficiency calculated by the functional dependence and mechanistic transport approach.

Nevertheless, the widely accepted hypothesis of fast surface reactions restricts the exploration of transport-chemistry interactions that govern complex phenomena like ignition. Specifically, modelling reaction kinetics based solely on mass transfer simplifies the modelling process but overlooks the recombination reaction taking place within the flow volume, and so the gas-phase ignition. To accurately capture this process, more detailed modelling approaches are required, incorporating chemical interactions in both the volume and on the surface. Although the proposed functional dependence (8) does provide with quite realistic PAR RVK-500 efficiency, this equation needs to be investigated in more detail.

4. Conclusions

The study aimed to investigate the performance and efficiency of cylindrical-type PAR catalyst in hydrogen recombination reactions, which are crucial for preventing hydrogen explosions in nuclear power plants and other industrial hydrogen facilities. Comprehensive analysis of a cylindrical-type catalyst has provided valuable insights into the PAR operational behaviour for hydrogen safety.

Experimental results showed that the cylindrical-type PAR catalyst is highly effective in recombining hydrogen and preventing the accumulation of flammable gas mixtures in the confined environment. Experimental results provide the total and local hydrogen concentrations at the outlet of recombiner channel. CFD results provide a detailed understanding of the flow patterns, concentration, and temperature profiles inside the recombiner channel and over catalyst section. The results were in good agreement with the experimental data. The study is investigated the effect of various operating parameters such as the inlet flow rate, hydrogen concentration, thermal diffusion (Soret effect), Schmidt number on the recombination efficiency and catalyst temperature. The turbulent Schmidt number was numerically calculated during addition CFD modelling in this paper. CFD results indicate that the Sc_t value within the range 0.2–0.28 allows for the best prediction of experimental temperature profiles of cylindrical-type PAR catalysts. Lastly, this paper proposes the functional dependence to estimate the efficiency of the entire PAR RVK-500 based on Sherwood equation and mechanistic transport approach.

Overall, the study has demonstrated the importance of understanding the behaviour and performance of cylindrical-type PAR catalysts in hydrogen safety systems. The results can be used to optimise the design and operation of PAR systems and improve their effectiveness and

reliability in preventing hydrogen explosions. The study also highlights the importance of combining experimental and computational approaches to gain a comprehensive understanding of the complex phenomena involved in hydrogen recombination reactions. Further parametric research is required, nonetheless, to investigate the performance of cylindrical-type PAR catalysts under different conditions.

CRediT authorship contribution statement

A.A. Malakhov: Conceptualization, Validation, Methodology, Investigation, Writing – original draft, Writing – review & editing, Visualization. **A.V. Avdeenkov:** Conceptualization, Investigation, Validation, Formal analysis, Writing – review & editing, Supervision, Project administration. **M.H. du Toit:** Methodology, Formal analysis, Resources, Writing – review & editing, Supervision. **Q.H. Duong:** Validation, Formal analysis, Writing – review & editing, Resources. **D.G. Bessarabov:** Writing – review & editing, Supervision, Project administration, Funding acquisition.

Declaration of competing interest

The authors declare that they have no known competing financial interests or personal relationships that could have appeared to influence the work reported in this paper.

Data availability

Data will be made available on request.

Acknowledgments

This work is based on the research supported in part by the HySA Infrastructure in South Africa, through their financial support [KP5 program], the Department of Science and Innovation (DSI), and National Research Foundation of South Africa through their grant [PSTD2203291140]. The authors also thank the Centre for High Performance Computing (CHPC) (South Africa) for computational resources used in this study.

Appendix A. Supplementary data

Supplementary data to this article can be found online at https://doi.org/10.1016/j.nucengdes.2023.112822.

References

Abe, J.O., Popoola, A.P.I., Ajenifuja, E., Popoola, O.M., 2019. Hydrogen energy, economy and storage: Review and recommendation. Int. J. Hydrogen Energy 44 (29), 15072–15086. https://doi.org/10.1016/j.ijhydene.2019.04.068.

Appel, C., et al., 2002. An experimental and numerical investigation of turbulent catalytically stabilized channel flow combustion of hydrogen/air mixtures over platinum. Proc. Combust. Inst. 29 (1), 1031–1038. https://doi.org/10.1016/S1540-7489(02)80130-4.

Arnould, F., et al. 2001. State of the Art on Hydrogen Passive Autocatalytic Recombiner. The International Conference on Nuclear Engineering, Nice, France 2001, 1(1), 1–23. Available at: (https://inis.iaea.org/search/search.aspx?orig_q=RN:33020098).

Avdeenkov, A.V., et al., 2018. Math hydrogen catalytic recombiner: Engineering model for dynamic full-scale calculations. Int. J. Hydrogen Energy 43 (52), 23523–23537. https://doi.org/10.1016/j.ijhydene.2018.10.212.

Avdeenkov, A.V., Kalyakin, S.G., Soloviev, S.L., Quang, H.D., 2022. On the scalability of the operating capacity of hydrogen recombiners. Nucl. Energy Technol. 8 (2), 143–152. https://doi.org/10.3897/nucet.8.8322.

Bezgodov, E., et al., 2022. Start-up behavior and the ignition limit of passive hydrogen recombiners with various catalytic elements. Nucl. Eng. Design 389 (Jan), 111664. https://doi.org/10.1016/j.nucengdes.2022.111664.

Blanchat, T.K., Malliakos, A.C., 1999. Analysis of hydrogen depletion using a scaled passive autocatalytic recombiner. Nucl. Eng. Design 187 (2), 229–239. https://doi.org/10.1016/S0029-5493(98)00283-0.

Blanchat, T.K., Malliakos, A.C., 2000. Testing a passive autocatalytic recombiner in the Surtsey facility. Nucl. Technol. 129 (3), 356–373. https://doi.org/10.13182/NT00-A3067.

Blocken, B., Stathopoulos, T., Saathoff, P., Wang, X., 2008. Numerical evaluation of pollutant dispersion in the built environment: Comparisons between models and experiments. J. Wind. Eng. 96 (10–11), 1817–1831. https://doi.org/10.1016/j.jweia.2008.02.049.

Botha, L.M., Ouma, C.N.M., Obodo, K.O., Bessarabov, D., 2023. Hydrogen and oxygen recombination reaction on Pt–Ni and Pt–Co based alloys using density functional theory. Surf. Sci. 736, 122354 https://doi.org/10.1016/j.susc.2023.122354.

Brachet, J.C., Lorette, C., Michaux, A., et al., 2014. CEA studies on advanced nuclear fuel claddings for enhanced accident tolerant LWRs fuel (LOCA and beyond LOCA conditions). In: Fontevraud 8 - Contribution of Materials Investigations and Operating Experience to LWRs' Safety, Performance and Reliability. September, p. 10.

CD-Adapco. 2020. SIEMENS Simcenter Star CCM+ User Guide, Version 2020.1; CD-Adapco: New York (USA).

Deutschmann, O., Schmidt, R., Behrendt, F., Warnatz, J., 1996. Numerical modeling of catalytic ignition. Symp. (Int.) Combust. 26 (1), 1747–1754. https://doi.org/10.1016/S0082-0784(96)80400-0.

Dogwiler, U., Benz, P., Mantzaras, J., 1999. Two-dimensional modelling for catalytically stabilized combustion of a lean methane-air mixture with elementary homogeneous and heterogeneous chemical reactions. Combust. Flame 116 (1–2), 243–258. https://doi.org/10.1016/S0010-2180(98)00036-4.

du Preez, S.P., Kozhukhova, A.E., Bessarabov, D.G., 2022. Catalytic hydrogen combustion using platinum supported on anodized aluminium oxide adhered to metallic aluminium. S. Afr. J. Chem. 76, 31–37. https://doi.org/10.17159/0379-4350/2022/v76A06.

du Toit, M., Chirayath, S., 2015. Proposal for improved nuclear fuel utilisation and economic performance by utilising thorium. J. Energy Southern Africa 26 (2), 11–18. https://doi.org/10.17159/2413-3051/2015/v26i2a2191.

du Toit, M.H., Naicker, V.V., 2018. Neutronic design of homogeneous thorium/uranium fuel for 24 month fuel cycles in the European pressurized reactor using MCNP6. Nucl. Eng. Des. 337, 394–405. https://doi.org/10.1016/j.nucengdes.2018.07.023.

duToit, M.H., Avdeenkov, A.V., Bessarabov, D.G., 2018. Reviewing H_2 Combustion: A case study for non-fuel-cell power systems and safety in passive autocatalytic recombiners. Energ. Fuel. 32, 6401–6422. https://doi.org/10.1021/acs.energyfuels.8b00724.

Frank-Kameneckij D.A., Diffusion and heat exchange in chemical kinetics: translation By N. Thon. – Princeton University Press, 1955.

Gardner, L.B., et al., 2021. Hydrogen recombination scaling experiments at CNL's hydrogen safety test facility. Nucl. Eng. Des. 377 (Feb), 111152 https://doi.org/10.1016/j.nucengdes.2021.111152.

Gardner, L.B., Marcinkowska, K., 2012. AECL passive autocatalytic recombiners. Canadian Nucl. Soc. Bull. 1 (33), 35–39.

Gasparyan, M.D., et al., 2015. Application of high-porosity ceramic block-cellular palladium catalysts in the oxidation of hydrogen isotopes. Glass Ceram. (english Translation of Steklo i Keramika) 71 (11–12), 396–399. https://doi.org/10.1007/s10717-015-9696-4.

Gera, B., Sharma, P.K., Singh, R.K., 2010. Numerical study of passive catalytic recombiner for hydrogen mitigation. CFD Lett. 2 (3), 123–136.

Gupta, S., Kanzleiter, T., Poss, G. 2015. Passive autocatalytic recombiners (PAR) induced ignition and the resulting hydrogen deflagration behaviour in lower containments. Conference: The 16th International Topical Meeting on Nuclear Reactor Thermal Hydraulics (NURETH-16), Chicago, IL, USA, 30.

Huang, X.G., Yang, Y.H., Zhang, S.X., 2011. Analysis of hydrogen risk mitigation with passive autocatalytic recombiner system in CPR1000 NPP during a hypothetical station blackout. Ann. Nucl. Energ. 38 (12), 2762–2769. https://doi.org/10.1016/j.anucene.2011.08.022.

Hunt, G., Karimi, N., Torabi, M., 2018. Two-dimensional analytical investigation of coupled heat and mass transfer and entropy generation in a porous, catalytic microreactor. Int. J. Heat and Mass Transf. 119, 372–391. https://doi.org/10.1016/j.ijheatmasstransfer.2017.11.118.

IEA. 2020. Energy Technology Perspectives 2020. (doi: 10.1787/ab43a9a5-en).

Keller, V.D., 2007. Passive catalytic hydrogen recombiners for nuclear power stations. Therm. Eng. 54 (3), 236–239. https://doi.org/10.1134/S0040601507030111.

Kelm, S., Jahn, W., Reinecke, E.A., 2008. Operational behaviour of catalytic recombiners—experimental results and modelling approaches. In: Proceedings of the Workshop on Experiments and CFD Code Application to Nuclear Reactor Safety (XCFD4NRS), pp. 10–12.

Kim, J., Hong, S., Park, K.H., Kim, J.H., Oh, J.Y., 2020. Experimental study on a hydrogen stratification induced by PARs installed in a containment. Energies 13 (21), 5552. https://doi.org/10.3390/en13215552.

Kim, C.H., Sung, J.J., Ha, S.J., Yeo, I.S., 2015. Implementation of passive autocatalytic recombiner system as a hydrogen mitigation system in Korean nuclear power plants. Atw. Internationale Zeitschrift Fuer Kernenergie 60 (8–9), 512–516.

Kirillov, I.A. 2022. Passive autocatalytic recombiners as explosion prevention and mitigation tool in hydrogen energy and transport infrastructures. Chem. Eng. Trans. 90 (Dec 2021) 127–132. (doi: 10.3303/CET2290022).

Klauck, M., et al. 2014. Passive auto-catalytic recombiners operation in the presence of hydrogen and carbon monoxide: Experimental study and model development. Nucl. Eng. Des. 266 (Oct 2013) 137–147. (doi: 10.1016/j.nucengdes.2013.10.021).

Kozhukhova, A.E., du Preez, S.P., Bessarabov, D.G., 2019. Preparation of anodized aluminium oxide at high temperatures using low purity aluminium (Al6082). Surf. Coat. Technol. 378 (Aug), 124970 https://doi.org/10.1016/j.surfcoat.2019.124970.

Kozhukhova, A.E., Du Preez, S.P., Shuro, I., Bessarabov, D.G., 2020. Development of a low purity aluminum alloy (Al6082) anodization process and its application as a platinum-based catalyst in catalytic hydrogen combustion. Surf. Coat. Technol. 404, 126483 https://doi.org/10.1016/j.surfcoat.2020.126483.

Kozhukhova, A.E., du Preez, S.P., Malakhov, A.A., Besserabov, D.G., 2021a. A thermally conductive Pt / AAO catalyst for hydrogen passive autocatalytic recombination. Catalysts 11 (4), 1–25. https://doi.org/10.3390/catal11040491.
Kozhukhova, A.E., du Preez, S.P., Bessarabov, D.G., 2021b. Catalytic hydrogen combustion for domestic and safety applications: A critical review of catalyst materials and technologies. Energies 14 (16), 4897. https://doi.org/10.3390/en14164897.
Kozhukhova, A.E., du Preez, S.P., Bessarabov, D.G., 2022. Preparation of Pt/Ce–Zr–Y mixed oxide/anodized aluminium oxide catalysts for hydrogen passive autocatalytic recombination. In. J. Hydrogen Energy 47 (25), 12726–12738. https://doi.org/10.1016/j.ijhydene.2022.01.246.
Liang, Z., Gardner, L., Clouthier, T., Thomas, B., 2016. Experimental study of effect of ambient flow condition on the performance of a passive autocatalytic recombiner. Nucl. Eng. Des. 301, 49–58. https://doi.org/10.1016/j.nucengdes.2016.03.005.
Ljungström, S., Kasemo, B., Rosen, A., Wahnström, T., Fridell, E., 1989. An experimental study of the kinetics of OH and H2O formation on Pt in the H2 + O2 reaction. Surf. Sci. 216 (1–2), 63–92. https://doi.org/10.1016/0039-6028(89)90644-4.
Maestre, V.M., Ortiz, A., Ortiz, I., 2021. Challenges and prospects of renewable hydrogen-based strategies for full decarbonization of stationary power applications. Renew. Sustain. Energy Rev. 152, 111628 https://doi.org/10.1016/j.rser.2021.111628.
Malakhov, A.A., Avdeenkov, A.V., Du Toit, M.H., Bessarabov, D.G., 2020a. CFD simulation and experimental study of a hydrogen leak in a semi-closed space with the purpose of risk mitigation. Int. J. Hydrogen Energy 45 (15), 9231–9240. https://doi.org/10.1016/j.ijhydene.2020.01.035.
Malakhov, A.A., Du Toit, M.H., du Preez, S.P., Avdeenkov, A.V., Bessarabov, D.G., 2020b. Temperature profile mapping over a catalytic unit of a hydrogen passive autocatalytic recombiner: An experimental and computational fluid dynamics study. Energ. Fuel. 34 (9), 11637–11649. https://doi.org/10.1021/acs.energyfuels.0c01582.
Malakhov, A.A., Du Toit, M.H., Avdeenkov, A.V., Bessarabov, D.G., 2022. Study of the efficiency of a PAR Pt catalyst and CFD verification of detailed mechanism of H2/O2 oxidation. Nureth-19 25, 1–15.
Malakhov, A.A., Avdeenkov, A.V., Du Toit, M.H., Duong, Q.H., Bessarabov, D.G., 2023. Numerical study of thermal diffusion in a passive autocatalytic recombiner: Possible effects on catalyst temperature and hydrogen distribution. Int. J. Hydrogen Energy 48 (32), 12129–12138. https://doi.org/10.1016/j.ijhydene.2022.09.136.
Mantzaras, J., Bombach, R., Schaeren, R., 2009. Hetero-/homogeneous combustion of hydrogen/air mixtures over platinum at pressures up to 10 bar. Proc. Combust. Inst. 32 II(2), 1937–1945. https://doi.org/10.1016/j.proci.2008.06.067.
Meynet, N., Bentaib, A., 2012. Numerical study of hydrogen ignition by passive autocatalytic recombiners. Nucl. Technol. 178 (1), 17–28. https://doi.org/10.13182/NT12-A13544.
Meynet, N., Bentaïb, A., Giovangigli, V., 2014. Impact of oxygen starvation on operation and potential gas-phase ignition of passive auto-catalytic recombiners. Combust. Flame 161 (8), 2192–2202. https://doi.org/10.1016/j.combustflame.2014.02.001.
Mueller, M.A., Kim, T.J., Yetter. R.A., Dryer, F.L. 1999. Flow reactor studies and kinetic modeling of the H_2/O_2 reaction. Int. J. Chemical Kinet. 31(2), 113–125. (doi: 10.1002/(SICI)1097-4601(1999)31:2<113::AID-KIN5>3.0.CO;2-0).
Orszulik, M., Fic, A., Bury, T., 2015. CFD modeling of passive autocatalytic recombiners. Nukleonika 60 (2), 347–353. https://doi.org/10.1515/nuka-2015-0050.
Paladino, D., Andreani, M., Zboray, R., Dreier, J., 2012. Toward a CFD-grade database addressing LWR containment phenomena. Nucl. Eng. Des. 253, 331–342. https://doi.org/10.1016/j.nucengdes.2011.08.064.
Park, J.W., Koh, B.R., Suh, K.Y., 2011. Demonstrative testing of honeycomb passive autocatalytic recombiner for nuclear power plant. Nucl. Eng. Des. 241 (10), 4280–4288.
Prabhudharwadkar, D.M., Aghalayam, P.A., Iyer, K.N., 2011. Simulation of hydrogen mitigation in catalytic recombiner: Part-I: Surface chemistry modelling. Nucl. Eng. Des. 241 (5), 1746–1757. https://doi.org/10.1016/j.nucengdes.2010.09.032.
Raman, R.K., Iyer, K.N., Ravva, S.R., 2020. CFD studies of hydrogen mitigation by recombiner using correlations of reaction rates obtained from detailed mechanism. Nucl. Eng. Des. 360 (Jan), 110528 https://doi.org/10.1016/j.nucengdes.2020.110528.
Rehm, T.E., 2023. Advanced nuclear energy: the safest and most renewable clean energy. Curr. Opin. Chem. Eng. 39, 100878 https://doi.org/10.1016/j.coche.2022.100878.
Reinecke, E.A., et al., 2005. Modelling of catalytic recombiners. Comparison of REKO-DIREKT calculations with REKO-3 experiments. International Conference of Nuclear Energy for New Europe 2005. Available at: (https://arhiv.djs.si/proc/bled2005/htm/pdf/00092.pdf.
Reinecke, E.A., et al., 2010. Open issues in the applicability of recombiner experiments and modelling to reactor simulations. Prog. Nucl. Energy 52 (1), 136–147. https://doi.org/10.1016/j.pnucene.2009.09.010.
Reinecke, E.A., Tragsdorf, I.M., Gierling, K., 2004. Studies on innovative hydrogen recombiners as safety devices in the containments of light water reactors. Nucl. Eng. Des. 230 (1–3), 49–59. https://doi.org/10.1016/j.nucengdes.2003.10.009.
Reynolds, A.J., 1975. The prediction of turbulent Prandtl and Schmidt numbers. Int. J. Heat Mass Transf. 18 (9), 1055–1069. https://doi.org/10.1016/0017-9310(75)90223-9.
Rinnemo, M., Deutschmann, O., Behrendt, F., Kasemo, B., 1997. Experimental and numerical investigation of the catalytic ignition of mixtures of hydrogen and oxygen on platinum. Combust. Flame 111 (4), 312–326. https://doi.org/10.1016/S0010-2180(97)00002-3.
Rozeń, A., 2015a. A mechanistic model of a passive autocatalytic hydrogen recombiner. Chem. Process. Eng. 36 (1), 3–19. https://doi.org/10.1515/cpe-2015-0001.
Rozeń, A., 2015b. Modelling of a passive autocatalytic hydrogen recombiner - A parametric study. Nukleonika 60 (1), 161–169. https://doi.org/10.1515/nuka-2015-0002.
Rozeń, A., 2018. Simulation of start-up behaviour of a passive autocatalytic hydrogen recombiner. Nukleonika 63 (2), 27–41. https://doi.org/10.2478/nuka-2018-0004.
Shukla, V., et al. 2021. Development and validation of CFD model for catalytic recombiner against experimental results. Chem. Eng. J., 407 (Aug 2020), 127216. (doi: 10.1016/j.cej.2020.127216).
Sitar, J.V.L., et al., 1997. Qualification of passive autocatalytic recombiners for post-LOCA hydrogen mitigation in CANDU stations. Proceedings - Annual Conference, Canadian Nuclear Association 00–09.
Steffen, P.M., et al., 2017. Operational behavior of a passive auto-catalytic recombiner under low pressure conditions. Fusion Eng. Des. 124, 1281–1286. https://doi.org/10.1016/j.fusengdes.2017.02.019.
Tarasov, O.V., et al., 2017. Development and verification of a model of RVK-500,-1000 recombiners for modeling the containment shells of NPP with VVER by computational hydrodynamics. At. Energ. 121, 166–172. https://doi.org/10.1007/s10512-017-0178-3.
Tietsch, W., et al., 2010. Integrated hydrogen control solutions for severe accidents using passive autocatalytic recombiners. 21st International Conference Nuclear Energy for New Europe.
Tominaga, Y., Stathopoulos, T., 2007. Turbulent Schmidt numbers for CFD analysis with various types of flowfield. Atmos. Environ. 41 (37), 8091–8099. https://doi.org/10.1016/j.atmosenv.2007.06.054.
Warnatz, J., Allendorf, M.D., Kee, R.J., Coltrin, M.E., 1994. A model of elementary chemistry and fluid mechanics in the combustion of hydrogen on platinum surfaces. Combust. Flame 96 (4), 393–406. https://doi.org/10.1016/0010-2180(94)90107-4.
Zhang, X., Savara, A., Getman, R.B., 2020. A method for obtaining liquid-solid adsorption rates from molecular dynamics simulations: Applied to methanol on Pt (111) in H2O. J. Chem. Theor. Comput. 16 (4), 2680–2691. https://doi.org/10.1021/acs.jctc.9b01249.

Alexander A. Malakhov obtained his Engineer-Physics degree in Nuclear Engineering in 2013 from Moscow Engineering Physics Institute (MEPI), Russia, and then worked for I.I. Leypunsky Institute of Physics and Power Engineering. He obtained Ph.D degree in Chemical Engineering in 2022 from North West University (NWU), South Africa and currently enrolled as Post-Doctoral Fellow at HySA Infrastructure, NWU, South Africa. His research focuses on nuclear technologies, CFD modelling of hydrogen catalytic combustion and electrolysis.

Alexander V. Avdeenkov obtained his Ph.D. in Physics and Mathematics from Institute of Physics and Power Engineering, Russia. He is currently enrolled as Director of Innovation Technology at «All-Russian Research Institute for Nuclear Power Plants Operation» JSC ("VNIIAES JSC"), Extraordinary Professor at HySA Infrastructure, NWU, South Africa. His research experience is wide, including nuclear, atomic, molecular and optic physics with use of quantum-mechanical methods. He also works in the field of quantum chemistry, computer simulations of fuel-cells, hydrogen storage and material science.

Maria H. du Toit obtained her B.Eng in Chemical Engineering in 2010, and M.Eng in Nuclear Engineering in 2013, and then a Ph.D degree in Nuclear Engineering in 2017 from North-West University (NWU), South Africa. She is currently enrolled as Associate Professor along with post-graduate supervision and teaching at Mechanical Engineering Faculty, NWU, South Africa. Her work experience is varied, including nuclear energy and safety analysis, renewable energy sources, hydrogen catalytic combustion.

Huong Q. Duong obtained his Engineer-Physics degree in Nuclear Engineering in 2017 from Moscow Engineering Physics Institute (MEPI), Russia, and then enrolled as Ph.D student at Moscow Engineering Physics Institute (MEPI), Currently he works as Leading Engineer at Obninsk Institute for Nuclear Power Engineering. His research focuses on nuclear technologies, CFD modelling of hydrogen catalytic combustion.

Dmitri G. Bessarabov obtained his PhD in Chemistry specialising in membrane technology for gas separation. In 2001 he joined Aker Kvaerner Chemetics in Vancouver, Canada, to work in membrane technology. In 2006 he joined Ballard Power Systems in Canada where he was leading an R&D group on MEA Integration and Evaluation. He is currently enrolled as Director of DSI National Center of Competence HySA Infrastructure. His professional interest is including fuel cells, PEM electrolysis, hydrogen energy and storage, membranes, separations, applied electrochemistry, applied polymer science, environmental technologies, water treatment, post-graduate training in applied chemistry, international co-operation in membrane and electrochemical research.